Experimental Investigation on Deformation Behavior of Circular Underground Opening in Hard Soil using a 3D Physical Model

Jinwei Fu[1], Mohammad Reza Safaei[2], Hadi Haeri[1], Vahab Sarfarazi[3]*, Mohammad Fatehi Marji[4,] Leige Xu[1], and Ali Arefnia[5]

1. School of Civil Engineering and Transportation, North China University of Water Resources and Electric Power, Zhengzhou, China
2. School of Civil Engineering, Aria University of Sciences and Sustainability, Tehran, Iran
3. Department of mining engineering, Hamedan University of technology, Hamedan, Iran
4. Department of Mine Exploitation Engineering, Faculty of Mining and metallurgy, Institute of Engineering, Yazd University, Yazd, Iran
5. Department of Geotechnics & Transportation, Faculty of Civil Engineering, Universiti Teknologi Malaysia, Skudai, Johor, Malaysia

Article Info

Abstract

In this work, the mechanical behavior of strata deformation due to drilling and surface loading is investigated using a 3D physical model. For this purpose, a scaled-down physical model is first designed. Then the tunnel drilling and support system are built. The subsidence experiments performed due to tunnel excavation and loading in a very dense and loose soil are performed. Soil is clayey sand (SC), and the percentages of its components are as sand (S = 1. 41%), gravel (G = 25%), and clay (C = 9.33%). Unstable tunnel support experiments are also carried out using physical simulation. Finally, deformations of soil surface and subsidence of strata are observed and recorded. In the tunnel with segmental support, 18.75% more load is applied than in the unsupported tunnel, and the total subsidence of the strata is reduced by 36.2%. The area of the deformed inner layers is decreased by 74.2%, and the length of the affected area in the largest layer is decreased by 48%. The depth of the cavity created at the surface is 46.66% less.

1. Introduction

In the engineering applications of infrastructures, it is always necessary to visualize the mechanical behaviors of geo-material structures during their failure and collapse processes. Tunneling and underground spaces have found valuable engineering desires in the modern world due to the rise in populations, the environmental problems, and the lake of sufficient surface lands in the big cities. Therefore, the induced stresses during the excavation of underground structures and their effects on the surrounding civil constructions are of most importance to be analyzed [1]. Most of the underground excavations such as tunnels are built near the surfaces, and considered as shallow underground structures. In many cases, they are built in big cities and in soft formations [2]. However, soft ground formations have many

inherent difficulties for making the proper and safe tunnels in urban areas. Therefore, several empirical, physical, and numerical methods have been proposed by many researchers to study the issues related to tunneling in soft grounds. They presented some advantages and disadvantages of the proposed methods based on the collected data from laboratories, field measurements, and back-analyses. The problems related to the ground excavations, tunnel instabilities, surface settlements, reinforcement, and lining of tunnels are also discussed by these researchers [3-6]. The limitation here is that these methods generally do not resemble the 3D nature of the tunnel as construction progress, and also assume plain strain conditions [1]. However, the complete field investigation sometime is also not possible due to

✉ Corresponding author: vahab.sarfarazi@gmail.com (V. Sarfarazi).

some safety concerns that prevent to reach the tunnel collapse zone, expensive instrumentation (to monitor the deformational behavior), etc. On the other hand, the numerical method allows the researchers to do more realistic simulation of real-life complex tunnel models, which helps the users to monitor 3D face effects, tunnel lining interaction, and to develop excavation sequence stages [4, 6-17]. However, these numerical results were sometimes very difficult to interpret [1]. In addition, full-scale experiments were very expensive, time-consuming, problematic to run, and also hard to repeat. Due to these reasons, the deformational behavior of the circular underground opening in soft ground is analyzed using a scale down 3D physical model that has now become a powerful and versatile technique for studying various geotechnical problems. Messerli et al. [18] have employed a physical modelling technique to investigate the face failure mechanism for shallow circular opening that was excavated in a dry, cohesionless soil, and analyzes their experimental results with the help of limit equilibrium calculations. As reported by Mair et al. [4], tunnel induced settlement can be defined by a dimensionless parameter that is called "ground loss" or "volume loss". There are several relationships proposed by the researchers on ground surface settlements considering different effective parameters like overburden height, tunnel dimension, excavation method, and geotechnical strata [4, 19, 20]. These types of analytical methods are generally based on the assumption of elastic behavior of soil, and their application depends on the accuracy of their corresponding parameters. Peck [19] first suggested that the shape of a transverse surface settlement trough over a tunnel might approximate closely that governed by a Gaussian distribution curve or normal distribution curve obtained from the field measurement. Yang et al. [21] have introduced an analytical method based on the non-linear Mohr-Coulomb criteria to measure the supporting pressure on the quadrilateral tunnel. They used the modified tangential technique, the upper solution of supporting pressure for the shallow tunnel. They investigated the effect of lateral pressure coefficient, initial cohesion, uniaxial tension strength, overburden, and tunnel span. Fraldi et al. [22] have measured the collapsed zone area using the plasticity theory. They calculated the extension of the collapsed zone by the associated flow rule, and defined the plastic potential function coincided with the Hoek-Brown yield criterion. They then captured the geometry of the collapsed zone by

considering the Greenberg minimum principle. Mollon et al. [23] have introduced a 3D analytical method, a rotational failure mechanism to predict face pressure. They believed that the boundary of the collapsed zone in front of the tunnel face consisted of two logarithmic spirals. Ibrahim et al. [24] have extended this method to a layered ground with different friction angles. Similarly, Pan and Dias [25] have modified this method to cover non-circular tunnels. Among the analytical and experimental methods, there are several physical models conducted to investigate the supporting pressure. Lei et al. [26] have examined the effect of the dip of the ground surface on the supporting pressure. They built and tested a 1-g physical model with three different surface dip angles. They excavated the tunnel section in several steps, and recorded the amount of strain on the tunnel lining as well as applied pressure on it. Chen et al. [27] have conducted a physical model to measure the tunnel face pressure, and they did the test for three cover-to-tunnel diameter ratios. They simulated mechanized tunnel excavation using a 3D model. The tunnel face consisted of a rigid circular plate connected to a hydraulic jack that was capable of pushing back the face at a low rate. Moreover, they recorded the variation of pressure during displacement of the tunnel face. They defined the vertical and horizontal stress concentration coefficients. Based on the outcomes recorded by the pressure cells, buried around the tunnel, they obtained the loosened zone, arch crown, and arch foot through the amount of the previously mentioned coefficient [28-38].

In this work, the deformational behavior of circular underground opening in hard soil was investigated using a 3D physical model. The behavior of tunnels and deformations of soil, as a result of shear loading as well as tunnel excavation, in dense ground, for tunnels without maintenance and with segmental maintenance, were investigated using a 3D physical simulator.

2. Stages of construction and preparation of 3D physical model
2.2.1. Physical storage

The 3D physical model was made using seventeen corner pieces and separate belts of different sizes, two hollow acrylic transparent walls, and two glass walls, as well as three wooden boards and fourteen polystyrene sheets. The dimensions of the model, respectively, its length, height, and depth, are 75 cm x 75 cm x 25 cm; these dimensions are based on the Ratan et al.'s research

work [39]. The body of the tank is made of steel with five equal wings. 12 corner pieces with different sizes of 75 cm and 25 cm are connected to each other using welding joints. In order to strengthen the body of the model, 3 straps are welded under the wooden floor board and 2 other straps are welded in the wall of the tank. In order to observe and record the phenomena caused by the tests inside the soil, two flexible transparent screens have been used in the front and back of the

model (acrylic screens). Two holes have been created in the front and back walls of the tank to carry out the tunnel digging operation and related tests. In order to create a flexible boundary condition on the sides of the model, 14 polystyrene sheets were placed on its two sides, and to maintain their rigidity, two wooden boards were placed in front of the polystyrene sheets. Figures 1 to 3 show the dimensions and components of the model, along with its details.

Figure 1. 3D physical model from the front view.

2.2.2. Tunnel maintenance system with its segments

According to the implementation points, the diameter of subway tunnels is approximately 10 m, so the diameter of the hole created in the test model has a scale of 1 to 100. For tunnels with a diameter of 10 m, the segments with a thickness of 35 to 40 cm are usually used. The width of the segments is 1.5 m, on average (the advancing step of the segments). In cases where the waterproofing of the tunnel is of concern, the thickness of the segments is increased up to 60 cm. Considering the above information, the thickness of the segments was considered 40 cm in this research work (with a scale of 1/100, the thickness of the segments is 4 mm in the model). Taking into account the implementation points, the advancing length of each segment was chosen as 5.5 cm (considering

the limited dimensions of the tested sample, and also the possibility of soil infiltration from the many seams of the segments). Therefore, the segmentation method was used to maintain the tunnel. The dimensions and thickness of the segments should be defined according to the test but their diameter should not be larger than the diameter of the hole in the wall of the tank. For this purpose, integrated segments with an outer diameter of 10 cm, a length of 5.5 cm, and a thickness of 4 mm were made using cement-sand mortar. The framework was reinforced by steel and copper wires with a cross-sectional area of $1\ mm^2$, $6/0\ mm^2$, respectively, which are woven together in the form of a network. The standard cube sample filled with mortar used in the construction of segments showed a resistance equal to $256\ \dfrac{kg}{cm^2}$

after seven days of storage. By using this system, other tunnel maintenance methods can be selected and implemented according to the researcher's goal. Therefore, in this system, the researcher can change the characteristics of the resistance of the

segments and study the effect of each one. The construction of segments is removed if the tunnel does not require maintenance. In Figures 4 to 6, the images of segments and reinforcing reinforcements are given.

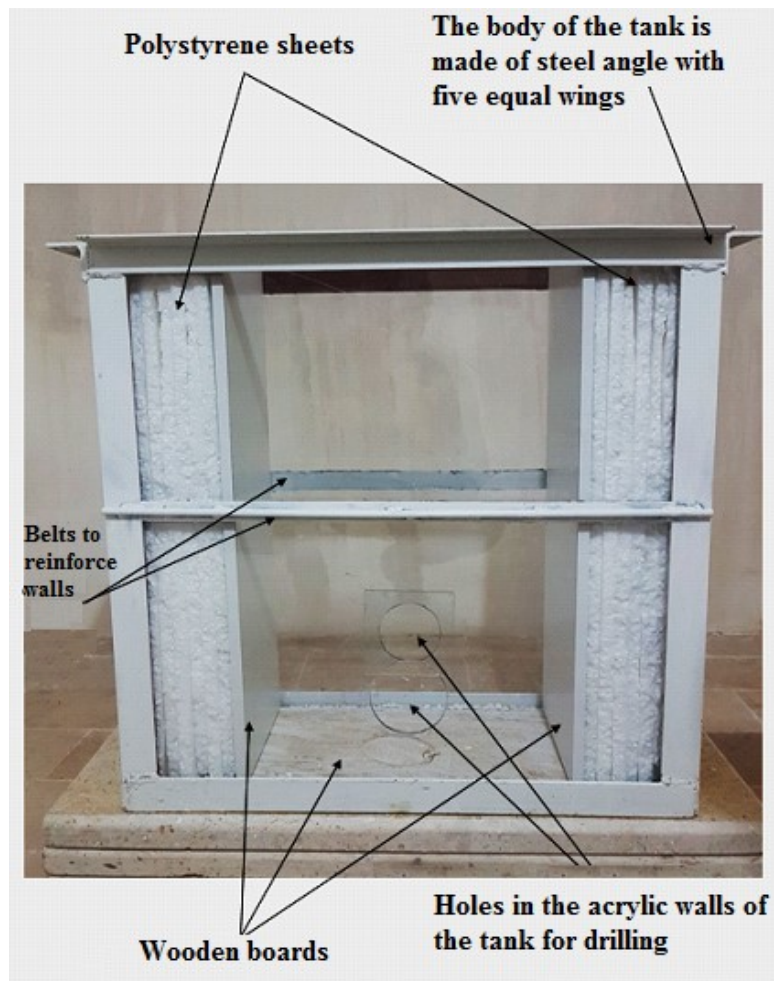**Figure 2. 3D physical model from side view.**

Figure 3. Components of physical model.

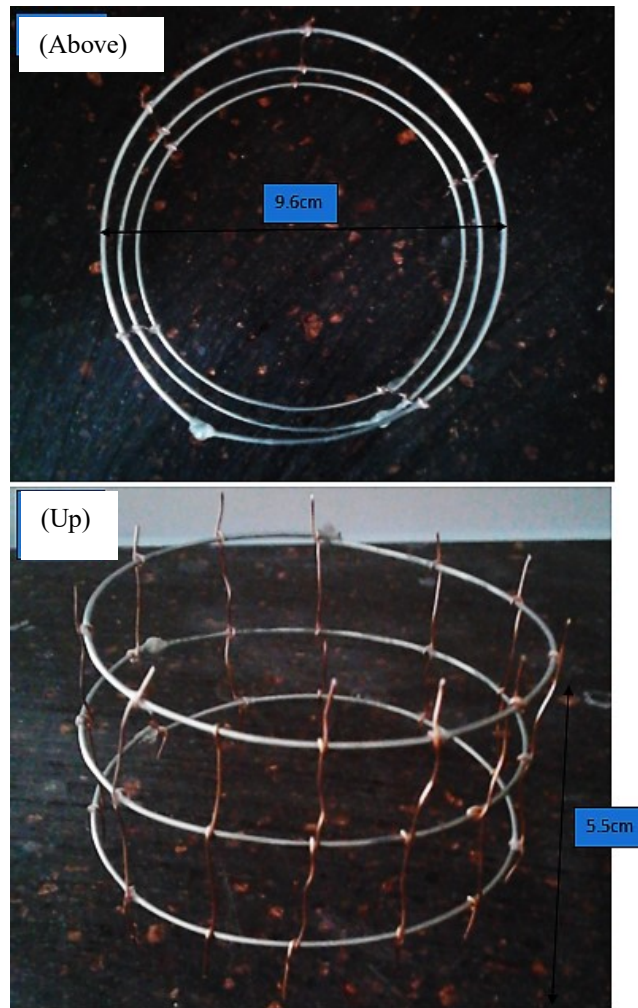**Figure 4. Side-view of segment.**

Figure 5. Armatures arming segments.

Figure 6. Dimensions of segments.

2.2.3. Tunnel excavation system

In order to simulate a system that works similar to a mechanized TBM machine, a 25 cm long steel drill was machined and manufactured for high-speed rotation and good balance when turning. The driving force of this drilling system is a dimmed drill with the ability to adjust the distance, which moves the drill. The drilling operation is performed by applying pressure from the back. In this system, it is possible to change the drilling method. If the drilling methods are studied, many changes can be applied, and the effect of each one can be checked and recorded. Therefore, the researcher can choose or make a drill according to the purpose of his experiment.

2.2.4. Soil studies

The geotechnical tests of the soil used in this study showed that the soil was clayey sand (SC), and the percentages of its components are as: sand (S = 1.41%), gravel (G = 25%) and clay (C =

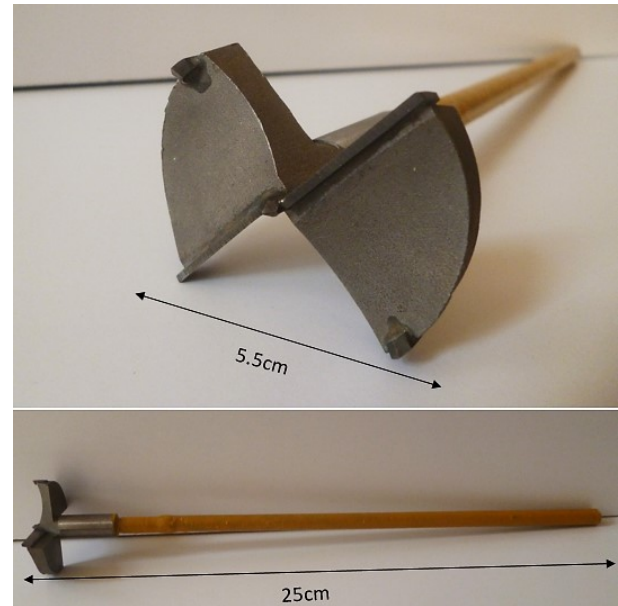9.33%). Table 1 gives the main characteristics of the soil.

Figure 7. TBM machine simulator drilling drill. An experiment to investigate settlement caused by tunnel excavation in very dense soil.

Table 1. Characteristics of the soil used in settlement test in dense soil.

Soil properties	Unit	Symbol	Value
Adhesion	$\frac{kg}{cm^2}$	C	0.8
Friction angle	degree	ϕ	32.8
specific gravity	-	G_s	2.67
Optimal humidity	-	ω_o	9.2%
Dry specific density	$\frac{kg}{cm^3}$	γ_d	2.03
Maximum specific density	$\frac{kg}{cm^3}$	γ_{dmax}	2.09
liquid limit	-	LL	28
plastic limit	-	PL	19
Plastic range	-	PI	9

The highest percentage of soil compaction is achieved when the optimal moisture content is $\omega_{0=}$%9.2, which is obtained from the compaction test results. In this test, water was added to the soil, i.e. 9.2% of the soil weight was water. After adding this required moisture, the soil was mixed well and used for the test.

In the standard compaction test (9.2% humidity), a force equal to $\frac{kg.f}{cm^2}$ 2.6 was applied during the test. To compact each layer of the soil with a

weight of 4 kg, which is released from a height of 15 cm, it is necessary to repeat this process 777 times. Therefore, for compacting 5 layers of the soil, this operation was repeated 3885 times, and it took three days to compact the soil. In order to better observe the settlement and its effect on different soil layers, white colored lines were created between the soil layers with neutral powder that did not stick. The number of white layers is five, and their distance from each other is 4 cm on average (Figure 8). The average thickness of each white layer is approximately 2 mm (Figure 9).

Figure 8. Creating white layers.

Figure 9. Five white layers created in physical tank (back-view).

On the outer part of the front and rear transparent walls of the physical model box, fixed blue lines were drawn that almost passed through the middle of the white layers. These blue lines are a good indicator for observing soil settlement and the change of the white layers corresponding to that settlement so that if the white layers that represent the soil layers are displaced and deformed, the amount of these displacements compared to the blue lines can be measured and observed. In addition, the upper and lower limits of the white layers were also marked with dots to increase the accuracy of the displacements (Figure 10).

Figure10. Six blue indicator lines on wall of physical model (rear- view).

Modeling in this physical simulation is done with a scale of 1/100. In one of the Ratan et al.'s experiments, the height of the tunnel arch to the ground level is 15 cm. In the upcoming research work, the depth of the tunnel is considered to be 15 cm; this height is 15 m in real scale. A large number of subway and urban transport tunnels are also dug

and built at this distance from the ground [38]. Before the start of drilling, the segments were polished to create the smallest seam in the rings of the segment during the fastening. Drilling was started by using the drill (which has already been described) and by using the driving force of a diamond drill with a low speed (Figure 11).

Figure 11. Drilling hole in front wall of physical model and soil before drilling.

At the beginning of drilling, in order to control the force applied to the drill bit, its rotation direction was considered counter-clockwise (Figure 12). After some digging and observing the stability of the soil and tunnel, the rotation direction of the drill and the direction of drilling operation were changed to increase the speed and progress. After a certain amount of digging, the soil was emptied manually. Segmentation was done simultaneously with drilling. The length of each step in the segmentation is approximately 1 cm. By applying pressure to the segments from the back, 1 cm of advance was created for each drilling step.

Figure 12. Mechanized drilling and simultaneous segmentation.

Using the same method of digging and maintaining the tunnel, progress was made to the end, and a 25 cm tunnel was dug inside the physical box sample. After each stage of drilling and segmentation, the condition of the soil was observed, and possible settlement was checked. It took three days to dig this tunnel (Figure 13).

Figure 13. End of drilling and segmentation.

2.2.5. Loading after drilling

In the first stage of loading, 16 kg loads were applied to the center of the tunnel. This loading remained for thirty days and nights. During this period, the physical box was modeled in vacuum and insulated so that the percentage of soil moisture did not change and the test results were not affected. Failure to observe the meeting after thirty days caused us to increase the load. For this purpose, eight kg concrete blocks were used. After adding each block, the possible conditions of soil deformations and settlements were checked. At this stage, the load increased to 64 kg (Figure 14). Finally, in the third step, to check the stability of the tunnel and the effects of the absence of segments, the maintenance of the tunnel was stopped and the segments were removed from the tunnel and the load increased to 200 kg. The final loading was left on the tunnel for 24 hours, after which the test was stopped.

Figure 14. Loading equivalent to 64 kg on tunnel maintained with segments.

3. Results
A) Failure patterns

In the tunnel excavation simulation test and settlement investigation, after the tunnel excavation, the loading gradually increased (with an increase rate of 8 kg in each stage); when the fourth piece of concrete block was added and the overhead weight reached 32 Kg, for the first time, collapse was observed inside the tunnel and some small pieces of soil fell from the tunnel arch to its floor. After loading the fifth piece of the block, the collapsed pieces became bigger and also the speed of these collapses increased. At this stage, some cracks were also created on the surface of the soil (Figure 15). Then with the loading of the last piece, the sixth concrete block with a weight of 48 kg, the speed and intensity of the fall reached its peak. The cracks that appeared on the surface of the soil were opened, and the weights that were used as surface structures sank into the soil and finally tilted and collapsed. The collapse of the tunnel continued until it was filled and completely destroyed (Figure 16).
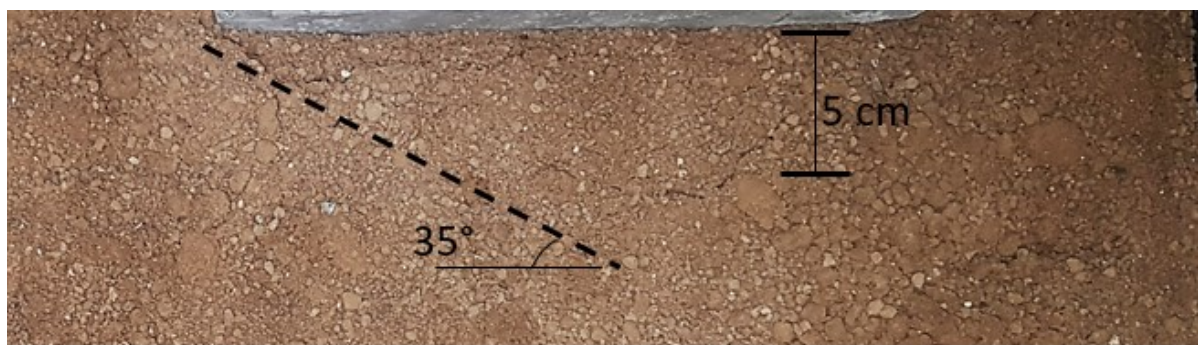

Figure 15. Cracks created on surface, crack opening, and soil failure.
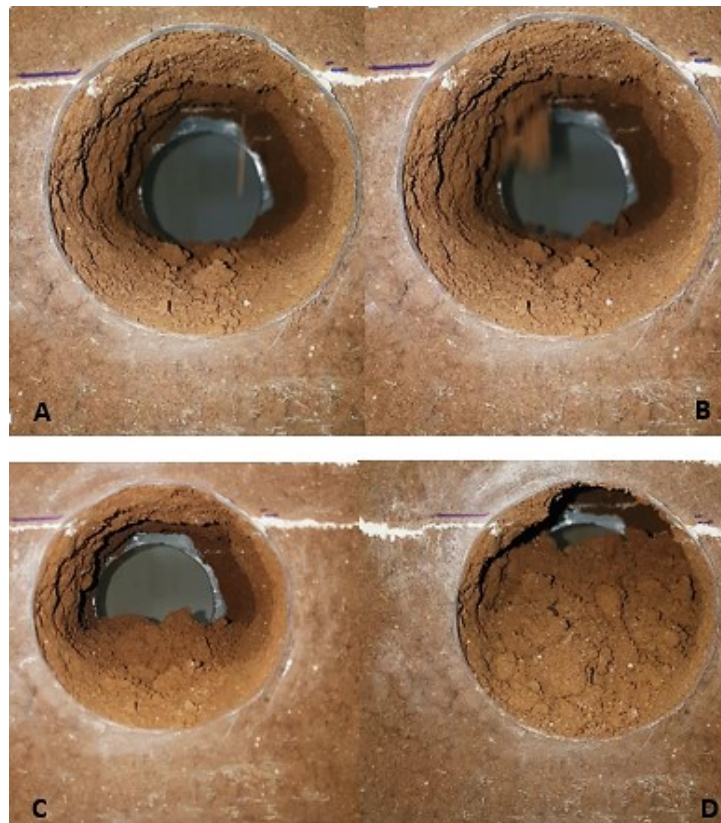
Figure 16. Stages of tunnel collapse.

As an indicator, blue lines were drawn on the transparent wall of the tank and corresponding to the center of the white soil layers. It was also marked with points around the top and bottom of the white layers on the wall. By using this technique, the displacements of the white layers can be observed and measured. Before loading, the blue indicator lines were on the white layers. After applying the load and settlement of the soil layers, the white layers that represent the layers of the earth were gradually changed, and the settlement was visible in them. This caused the white layers to move to the bottom of the indicator lines. This phenomenon is indicated in Figures 17 and 18.

The maximum vertical settlement of each white layer occurred in its middle. Therefore, as we move from the center of each layer to the sides, the settlement gradually decreases towards zero. Also as the layers became deeper, the settlement also increased, except for the seventh layer closed to the

tunnel. In this layer, less settlement was observed and recorded than the previous layer. Table 2 shows the maximum settlement in each layer.
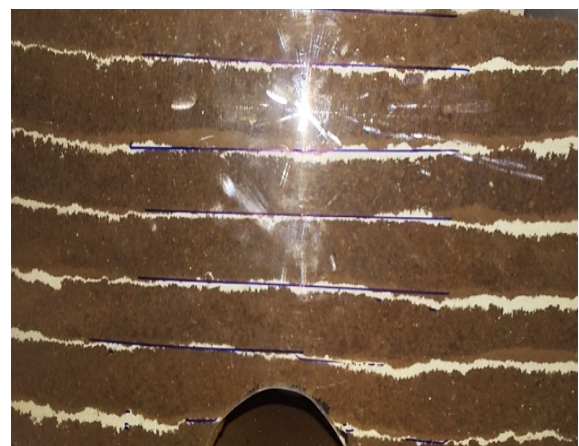

Figure 17. Blue indicator lines on white layers before settling.

Figure 18. Displacement of white layers relative to blue index lines after settlement (white layers came under index lines).

Table 2. Maximum settlement recorded in each layer.

Different layers of soil from surface to depth (white layers)	Maximum amount of vertical settlement in middle of layers in mm
First layer of soil surface	0.5
Second layer	1
Third layer	1.5
Fourth layer	3
Fifth layer	3.5
Sixth layer	4.5
Seventh layer	4

3.1. Maintenance and stabilization of collapsing tunnel with segmentation method

After the volume and speed of the falls increased and the tunnel became unstable and this process continued, it was decided to maintain the tunnel using the segmentation method (Figure 19). Therefore, segmentation was started and the soil poured into the tunnel was evacuated by wind pressure. The segments were aligned and fixed in place.

Figure 19. Maintenance and stabilization of collapsing tunnel with segmentation method.

After the end of this stage, the loading continued with an increase rate of half a kilogram. Concrete blocks gradually began to sink into the soil (Figure 20). When the overburden weight reached 70.5 kg, the blocks sank into the soil by an average of 7 mm. At this stage of loading, no crack was observed on the soil surface but for the first time, the settlement of the inner layers of the soil was observed and recorded.

The maximum leakage of each of the white layers is given in Table 3.

Figure 20. Blocks sinking into soil.

Table 3. Settlement recorded in center of white layers corresponding to load of 70.5 Kg.

Number of layers	Maximum settlement in center of each layer (mm)
First layer (soil surface)	0
Second layer	0
Third layer	0.5
Fourth layer	0.8
Fifth layer	1.7
Sixth layer	2.2
Seventh layer (next to tunnel)	1.7

After 11 minutes and without adding load, the depth of ground depression reached from 7 mm to 1 cm. However, the size of the land settlement did not change. When the load reached 78.5 kg, the depth of the pit also increased to 1.5 cm. The load continued to increase and when it reached 87 kg, the settlement in the white layers increased and reached a maximum of 3.5 mm for the sixth and seventh layers (Table 4).

By comparing Figures 21 and 22, the vertical movement of the soil layers and the settlement in the white layers can be seen.

Then the load continued to increase and reached 104 kg (Figure 23). At this stage and after the passage of five hours, only the depth of the pit increased to 2.3 cm, and there was no change in the settlement (Figure 24) and the tunnel remained stable.

Table 4. Settlement recorded in white layers corresponding to load of 87 Kg.

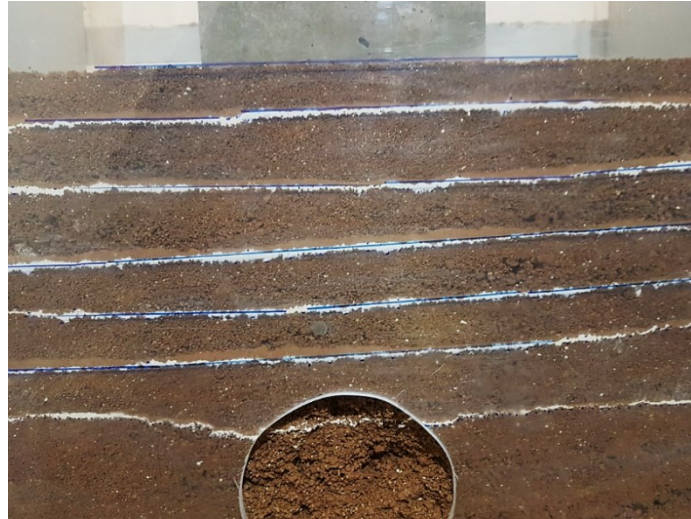| Number of layers	Maximum settlement in center of each layer (mm)
First layer (soil surface)	0
Second layer	0
Third layer	0.5
Fourth layer	1.5
Fifth layer	2.5
Sixth layer	3.5
Seventh layer (next to tunnel)	3.5

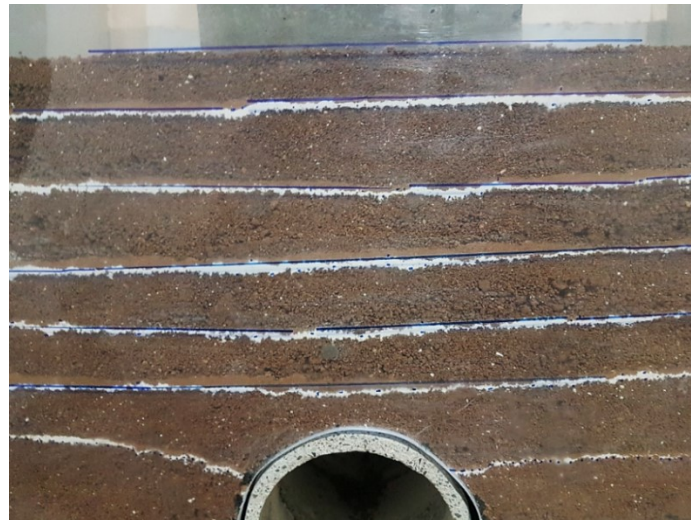**Figure 21. Placement of index lines on white layers before settling.**

Figure 22. Displacement of white layers relative to index lines after settlement.

Figure 23. Applying twelfth concrete block to tunnel with segmental maintenance.

Figure 24. Inside-view of tunnel during loading 104 kg and its stability.

The depth of the pit that was created due to sinking of weights (concrete blocks) on the ground is equal to 2.3 cm. Two cracks were observed in all four corners of the pit. Cracks were also created in the bottom of the pit, which were almost parallel to each other and in line with the length of the tunnel. Also there are two cracks on the surface of the ground almost in the center of the pit, which spread along the tunnel. The average length of these cracks is approximately 10 cm. In addition to that, the pit's square cracks spread deep into the ground so that it can be seen from behind the transparent walls of the model. The deepest of these vertical cracks penetrates to the third white layer and its length is 8.5 cm (Figures 25-27).

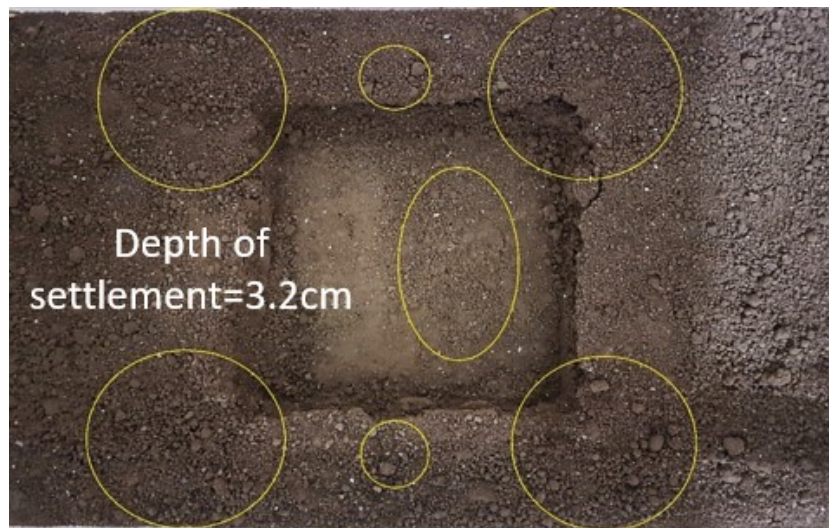In order to better observe the cracks, the black lines have been drawn and filled with color.

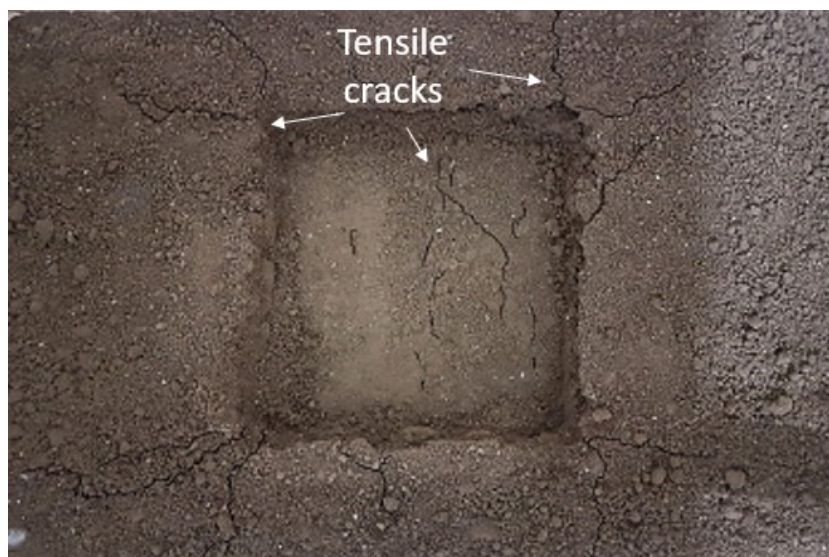**Figure 25. Areas where cracks have been created.**

Figure 26. Surface cracks caused by soil settlement and deformation.

Figure 27. Deepest vertical crack.

3.2. Removing segments, reloading until destroying tunnel

After the end of this phase of the test and the recording of its results, to continue the test, the segments were taken out of the tunnel and loading started again. The blocks were placed in the bottom of the pit that was created in the previous step. When the load reached 16 kg, a systematic collapse separated from the left wall of the tunnel. Then the load gradually increased to 40 kg. The drops of each stage of loading till reaching 40 kg are given in Figures 28(a-e).
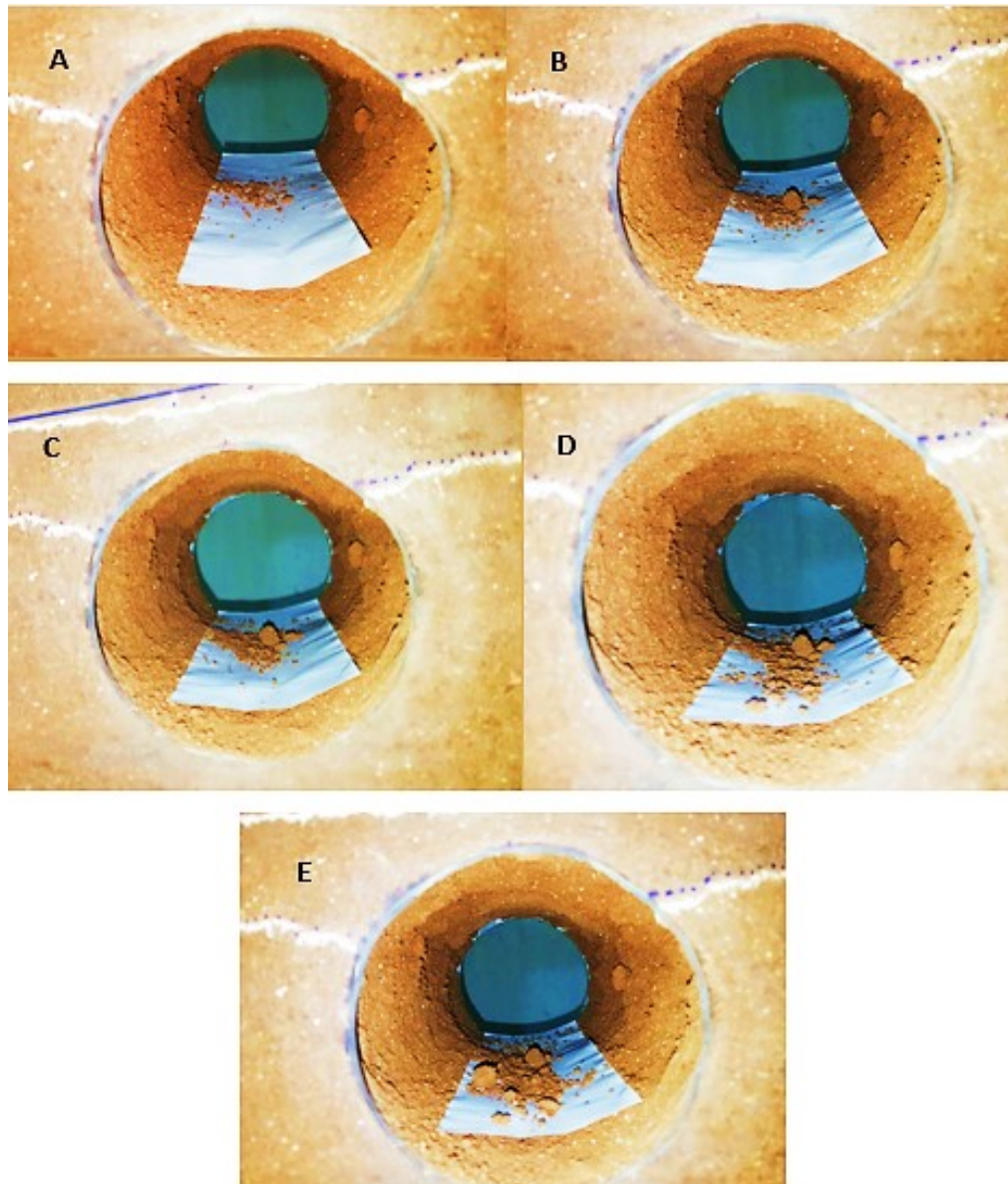
Figure 28. Drops caused by step loading, from 16 kg to 40 kg.

The load continued to increase. After the application of each weight, an instantaneous drop occurred and then the drop stopped (Figure 29). This is contrary to what has been observed so far (plastic spillage). When the tunnel load reached 70.6 kg, chain falls started at a rate of two seconds and it took fifty seconds for the rate of fall to decrease to seven seconds. After a while, the fall stopped. Finally, with a weight equal to 84 kg, the tunnel and overhead blocks both collapsed at the same time. The created pit has a depth of 5.8 cm. The settlements of the layers and the impact area were re-measured and no change was observed in them. The depth of the cracks created in the previous test did not increase either.

Figure 29. Pit after blocking the tunnel.

Figure 30. Collapse and blocking of tunnel.

Figure 31 compares the depths of the pit created on the soil surface for tunnel without maintenance and the tunnel maintained by segment.

The depth of the pit created by the overhead load of 47.45 kg in the tunnel without maintenance is equal to 6 cm, and the depth of the load pit in the segmental tunnel with the load of 103.6 kg is equal to 3.2 cm. The tunnel segment leads to decreasing the depth of pit. A comparison of the two is given in the image below (Figure 31).
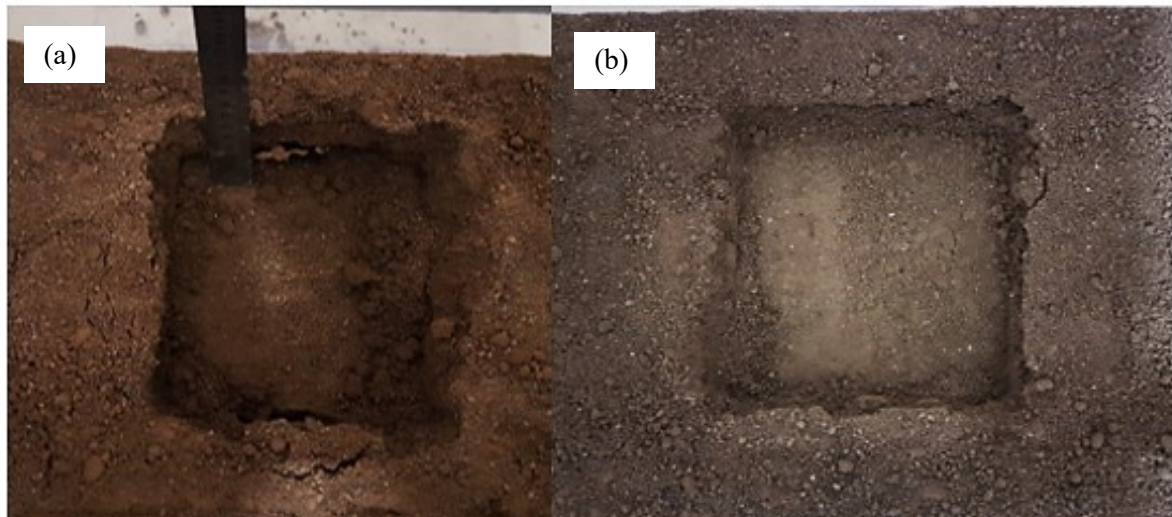
Figure 31. Comparison of depth of the pit created on soil surface a) tunnel without maintenance b) tunnel maintained by segment.

4. Conclusions

In this work, the behavior of tunnels and deformations of soil, as a result of shear loading as well as tunnel excavation, in dense ground, for tunnels without maintenance and with segmental maintenance, were investigated using a 3D physical simulator. The following main conclusions were obtained:

- The test of maintenance and stabilization of the unstable tunnel in loose ground, when the tunnel was protected using the segmental maintenance method was performed.

- A load equal to 104 kg was applied to the ground surface and the tunnel remained stable but when the tunnel was not maintained, it was destroyed with a load equal to 84 kg.

- The highest amount of settlement occurred in the upper and adjacent layers of the tunnel arch, and its value was 3.5 mm.

- The longest length that was deformed under the influence of settlement is related to the seventh layer and in the vicinity of the tunnel arch. In this layer, a range of 21.8 cm is placed under the radius, which is 2.18 times the diameter of the tunnel and 1.45 times the length of the loading blocks.

- The deep layers of the soil, which were deformed due to settlement, have an area equal to 109 cm^2, which is 1.39 times the area of the tunnel.

- The depth of the pit that was formed in the segmental tunnel due to the settlement of the inner layers of the soil and the collapse of the tunnel with a load of 104 kg is equal to 2.3 cm.

- The tunnel with a load between 80% and 77.7% of the final load led to collapse, destructive instability and progressive destruction.

- With the passage of time and the increase in load, the speed, intensity, and dimensions of the falling pieces inside the tunnel increased.

- In dense soils, the width of the sinkhole is equal to the diameter of the tunnel.

References

[1]. Meguid, M.A. Saada, O. Nunes, M.A. and Mattar, J. (2008). Physical modeling of tunnels in soft ground: A review. Tunn Undergr Sp Technol. 23 (2):185–98.

[2]. Idinger, G. Aklik, P. Wu, W. and Borja, RI. (2011). Centrifuge model test on the face stability of shallow tunnel. Acta Geotech. 6 (2):105–17.

[3]. Hoek, E. and Brown, E.T. (1980). Empirical Strength Criterion for Rock Masses. Vol. 106, Journal of the Geotechnical Engineering Division. pp. 1013–35.

[4]. Mair, R.J. Taylor, R.N. and Bracegirdle, A. (1993). Sub-surface settlement profiles above tunnels in clays. Géotechnique. 45 (2):361–2.

[5]. Hoek, E. and Diederichs, M.S. (2006). Empirical estimation of rock mass modulus. Int J Rock Mech Min Sci. 43 (2):203–15.

[6]. Kim, C. Baek, S. and Hong, S. (2005). Tunnel convergence analyses in heterogeneous/anisotropic rock masses. In: Yücel Erdem and Tülin Solak, editor.

International World Tunnel Congress and the 31st ITA General Assembly. Istanbul, Turkey; pp. 1091–7.

[7]. Pickhaver, J.A. (2006). Numerical Modelling of Building Response to Tunnelling. University of Oxford, Thesis (Ph.D.), uk.bl.ethos.437034.

[8]. Zhou, K. Xia, M. (2009). Numerical Modelling for Designing Tunnel Support in Heavily Jointed Rock. 2009 Int Conf Electron Comput Technol. 471– 4.

[9]. Juneja, A. Roshan, N.S. (2010). Study on tunnelling induced ground deformation in reinforced soils. Phys Model Geotech–6th ICPMG '06–Ng, Zhang &Wang © 2006 Taylor Fr Group, London.555–60.

[10]. Ma, L. Ding, L. and Luo, H. (2014). Non-linear description of ground settlement over twin tunnels in soil. Tunn Undergr Sp Technol. 42:144–51.

[11]. Hao, X.J. Feng, X.T. Yang, C.X. Jiang, Q. Li, S.J. (2015). Analysis of EDZ Development of Columnar Jointed Rock Mass in the Baihetan Diversion Tunnel. Rock Mech Rock Eng.43 (3):44-55.

[12]. Nikadat, N. Fatehi, M. and Abdollahipour, A. (2015). Numerical modelling of stress analysis around rectangular tunnels with large discontinuities (fault) by a hybridized indirect BEM. J Cent South Univ , 22 (11):4291–9.

[13]. Yang, F. Zhang, J. Yang, J. (2015). Stability analysis of unlined elliptical tunnel using finite element upper-bound method with rigid translatory moving elements. Tunn Undergr Sp Technol. 50:13–22.

[14]. Zhang, Z.X. (2016). Three-dimensional finite-element analysis on ground responses during twin-tunnel construction using the URUP method. Tunn Undergr Sp Technol Inc Trenchless Technol Res. 58:133–46.

[15]. Kiani, M. Akhlaghi, T. (2016). Experimental modeling of segmental shallow tunnels in alluvial affected by normal faults. Tunn Undergr Sp Technol. 51:108–19.

[16]. Wang, Y. (2017). Effect of a Fault Fracture Zone on the Stability of Tunnel-Surrounding Rock. Int J Geomech. 04016135:1-20.

[17]. Abdollahi, M.S. (2019). A 3D numerical model to determine suitable reinforcement strategies for passing TBM through a fault zone, a case study: Safaroud water transmission tunnel, Iran, Tunneling and Underground Space Technology 88, 186-199

[18]. Messerli, J. (2010). Experimental study into tunnel face collapse in sand. Phys Model Geotech. 1(1961):575–80.

[19]. Peck, R. (1969). Deep excavation and tunneling in soft ground. In: State of the Art Report. In: 7th International Conference on Soil Mechanics and Foundation Engineering. p. 225–90.

[20]. Sagasetta, C. (1987). Analysis of underground soil deformation due to the ground loss. Geotchhnique. 37(3):301–30.

[21]. Fraldi, M. and Guarracino, F. (2010). Analytical solutions for collapse mechanisms in tunnels with arbitrary cross sections. International Journal of Solids and Structures. 47 (2): 216-223.

[22]. Yang, X.L. Yang, Z.H. Li, Y.X. and Li, S.C. (2013). Upper bound solution for supporting pressure acting on shallow tunnel based on modified tangential technique. Journal of Central South University. 20 (12): 3676-3682.

[23]. Mollon, G. Dias, D. and Soubra, A.H. (2011). Rotational failure mechanisms for the face stability analysis of tunnels driven by a pressurized shield. International Journal for Numerical and Analytical Methods in Geomechanics. 35 (12): 1363-1388.

[24]. Ibrahim, E. Soubra, A.H. Mollon, G. (2015). Three-dimensional face stability analysis of pressurized tunnels driven in a multilayered purely frictional medium. Tunneling and Underground Space Technology, 49: 18-34.

[25]. Pan, Q. and Dias, D. (2017). Upper-bound analysis on the face stability of a non-circular tunnel. Tunnelling and Underground Space Technology, 62, 96-102.

[26]. Pan, Q. and Dias, D. (2017). Upper-bound analysis on the face stability of a non-circular tunnel. Tunnelling and Underground Space Technology, 62, 96-102.

[27]. Chen, R. P. (2013). Experimental study on face instability of shield tunnel in sand. Tunnelling and Underground Space Technology, 33, 12-21.

[28]. Yaylaci, M. Terzi, C. and Avcar, M. (2019). Numerical analysis of the receding contact problem of two bonded layers resting on an elastic half plane, Struct. Eng. Mech., 72 (6): 775-783.

[29]. Yaylaci, M. and Avcar, M. (2020). Finite element modeling of contact between an elastic layer and two elastic quarter planes, Comput. Concrete. 26 (2): 107-114.

[30]. Yaylaci, M., Adiyaman, E., Oner, E., and Birinci, A. (2020). Examination of analytical and finite element solutions regarding contact of a functionally graded layer, Struct. Eng. Mech. 76 (3): 325-336.

[31]. Yaylaci, M. Eyuboglu, A. Adiyaman, G. Uzun Yaylaci, E. O ner, E. and Birinci, A. (2021a). Assessment of different solution methods for receding contact problems in functionally graded layered mediums, Mech. Mater., 154, 103730.

[32]. Yaylaci, M. Yayli, M. Uzun Yaylaci, E. Olmez, H. and Birinci, A. (2021b). Analyzing the contact problem of a functionally graded layer resting on an elastic half plane with theory of elasticity, finite element method and multilayer perceptron, Struct. Eng. Mech., 78 (5): 585-597.

[33]. Gil., D.M. and Golewski, G.L. (2018). Effect of silica fume and siliceous fly ash addition on the fracture toughness of plain concrete in mode I, IOP Conf. Ser. Mater. Sci. Eng. 416 012065.

[34]. Golewski, G.L. (2018). An analysis of fracture toughness in concrete with fly ash addition, considering all models of cracking, IOP Conf. Ser. Mater. Sci. Eng, 416 012029

[35]. Golewski, G.L. (2019). Physical characteristics of concrete, essential in design of fracture-resistant, dynamically loaded reinforced concrete structures, Material Design and Processing Communications. 1 (5): 33-44.

[36]. Golewski, G.L. (2021). On the special construction and materials conditions reducing the negative impact of vibrations on concrete structures, Materials Today: Proceedings, 66-77.

[37]. Golewski, G.L. (2022). Strength and microstructure of composites with cement matrixes modified by fly ash and active seeds of CSH phase, Structural Engineering and Mechanics. 82 (4): 543-556.

[38]. Golewski, G.L. (2021). Application of the C-S-H phase nucleating agents to improve the performance of sustainable concrete composites containing fly ash for use in the precast concrete industry, Materials. 14 (21): 6514.

[39]. Das, R. Sirdesai, N.N. and Singh, T.N. (2017). Analysis of Deformational Behavior of Circular Underground Opening in Soft Ground Using Three-Dimensional Physical Model, the 51st US Rock Mechanics / Geomechanics Symposium held in San Francisco, California, USA, 25-28.

بررسی آزمایشگاهی رفتار تغییر شکل فضاهای زیرزمینی دایره‌ای مقطع در خاک سخت با استفاده از مدل فیزیکی سه بعدی

جین وی فو[1]، محمدرضا صفایی[2]، هادی حائری[1]، وهاب سرفرازی[3]*، محمد فاتحی مرجی[4]، لیگه خو[1] و علی عارف نیا[5]

۱- دانشکده مهندسی عمران و حمل و نقل، دانشگاه منابع آب و نیروی برق شمال چین، ژنگژو، چین

۲- دانشکده مهندسی عمران، موسسه آموزش عالی غیر دولتی غیر انتفاعی علوم و توسعه پایدار آریا، تهران ، ایران

۳- گروه مهندسی معدن، دانشگاه صنعتی همدان، همدان، ایران

۴- دانشکده معدن و متالورژی، مؤسسه فنی و مهندسی، دانشگاه یزد، یزد، ایران

۵- گروه ژئوتکنیک و حمل و نقل، دانشکده مهندسی عمران، دانشگاه تکنولوژی مالزی، اسکودای، جوهور، مالزی

چکیده:

در این مقاله رفتار مکانیکی تغییر شکل لایه‌ها در اثر حفاری و بارگذاری سطحی با استفاده از یک مدل فیزیکی سه بعدی بررسی شده است. برای این منظور ابتدا یک مدل فیزیکی کوچک مقیاس طراحی شد. سپس سیستم حفاری و نگهداری تونل ساخته شد. آزمایشات نشست در اثر حفر تونل و بارگذاری در خاک بسیار متراکم و سست انجام شد. در این مطالعه از خاک ماسه رسی (SC) استفاده شده است که درصد اجزای آن عبارتند از: ماسه (%1.41 = S)، شن (%25 = G) و خاک رس (%9.33 = C) . آزمایش‌های نگهداری تونل ناپایدار نیز با استفاده از شبیه‌سازی فیزیکی انجام شد. در نهایت تغییر شکل سطح خاک و نشست لایه‌های خاک مشاهده و ثبت شد. در تونل با پوشش بتنی پیش ساخته شده (سگمنتال) ، ۱۸٫۷۵ درصد بار بیشتری نسبت به تونل بدون نگهداری اعمال شد و نشست کل لایه ها ۳۶٫۲ درصد کاهش یافت. مساحت لایه های داخلی تغییر شکل یافته ۷۴٫۲ درصد کاهش و طول ناحیه تاثیر در بزرگترین لایه ۴۸ درصد کاهش یافت. عمق حفره ایجاد شده در سطح ۴۶٫۶۶ درصد کمتر بود.

کلمات کلیدی: مدل فیزیکی سه بعدی، نشست، تونل، حفاری، سگمنت.